

See discussions, stats, and author profiles for this publication at: <https://www.researchgate.net/publication/258717879>

Polarization switching of transverse modes in VCSELs subject to two-frequency orthogonal optical injection

Article in *Proceedings of SPIE - The International Society for Optical Engineering* · May 2012

DOI: 10.1117/12.922524

CITATIONS

0

READS

87

5 authors, including:



Ana Quirce

Instituto de Física de Cantabria- Universidad de Cantabria

69 PUBLICATIONS 664 CITATIONS

[SEE PROFILE](#)



Angel Valle

Universidad de Cantabria

200 PUBLICATIONS 2,608 CITATIONS

[SEE PROFILE](#)



Hong Lin

Bates College

53 PUBLICATIONS 255 CITATIONS

[SEE PROFILE](#)

Some of the authors of this publication are also working on these related projects:



VCSELs [View project](#)



Dynamics of VCSELs [View project](#)

Polarization switching of transverse modes in VCSELs subject to two-frequency orthogonal optical injection

A. Quirce^{1,2}, A. Valle^{1*}, H. Lin³, Y. Zhang³, and D. W. Pierce³.

¹Instituto de Física de Cantabria, CSIC-Universidad de Cantabria, Avda. Los Castros s/n, E-39005, Santander, Spain.

²Departamento de Física Moderna, Universidad de Cantabria, Avda. Los Castros s/n, E-39005, Santander, Spain

³Department of Physics & Astronomy, Bates College, Lewiston, ME 04240, USA.

ABSTRACT

We report a theoretical study of the polarization and transverse mode properties of single and multi-transverse mode VCSELs when they are subject to two-frequency, or dual-beam, orthogonal optical injection. We analyze the nonlinear dynamics of the system making special emphasis in the double injection locking observed at large injection strengths, useful for photonic microwave signal generation. Simulation of single and multi-transverse mode VCSELs show that the double injection locking can be obtained when these devices are subject to dual-beam orthogonal optical injection. We show that the extra degree of freedom given by the multi-transverse mode operation of the VCSEL under dual-beam orthogonal optical injection is useful for enhancing the performance of the photonic microwave generation system. In fact we obtain that the higher-order transverse mode is excited with a much larger amplitude than that of the fundamental transverse mode. The response of the multi-transverse mode VCSEL is enhanced with respect to that obtained with a similar single-transverse mode VCSEL subject to the same dual-beam orthogonal optical injection. Wide tuning ranges, beyond the THz region, and narrow linewidths are also demonstrated in our system.

Keywords: Semiconductor lasers, vertical-cavity surface-emitting laser (VCSEL), polarization switching, transverse modes, optical injection, photonic microwave generation, radio-over-fiber (RoF), nonlinear dynamics.

I. INTRODUCTION

Optical injection is a technique that is commonly employed to improve the performance of semiconductor lasers without modifying their design [1]. Attention has been paid recently on the effects of optical injection on an special type of semiconductor laser: the vertical-cavity surface-emitting laser (VCSEL) [2-15]. VCSELs have demonstrated many impressive characteristics, including low threshold current, single-longitudinal mode operation, circular beam profile and easy fabrication in large two-dimensional arrays [2]. Emission in multiple transverse modes is usually found in VCSELs [16] as a result of spatial-hole burning effect [17]. Furthermore, due to the surface emission and cylindrical symmetry VCSELs lack strong polarization anisotropy and may undergo polarization switching (PS) [18]. The lack of polarization anisotropies and the multi-transverse mode behaviour of VCSELs provide new features to the rich nonlinear dynamics induced by optical injection. Locking of the frequency of the injected (slave) VCSEL to the one of the injecting (master) laser has been shown for reduction of the VCSEL linewidth or for an enhancement of its modulation bandwidth [3-5]. Orthogonal optical injection in VCSELs, in which the polarization of the injected signal is perpendicular to that of the VCSEL, has received a lot of attention [6-18]. Pan *et al.* [6] showed that by increasing the injection strength, the VCSEL switched its polarization to that of the injected light. Most of these studies have been performed for single-transverse mode VCSELs [6-12]. The effect of orthogonal optical injection on multi-transverse mode VCSELs has been also recently studied, showing that PS can be induced in all the transverse modes [13-15]. Recent experimental work has demonstrated single-mode [19] and multimode [20] VCSEL-by-VCSEL optical injection locking. VCSEL-by-VCSEL injection has interest for obtaining integrated low-cost high-speed communication modules [19].

*e-mail: valle@ifca.unican.es; phone 34 942 201465; fax: 34 942 200935

Nonlinear dynamics of optically injected semiconductor lasers can also be used for photonic microwave generation [21-28]. Compared with conventional microwave generation by electronic circuitry with multiple stages of frequency doubling, photonic microwave signal generation have the advantages of lower cost, longer transmission distance, less system complexity and the ability to generate tunable microwave signals with higher frequencies [23],[27]. Photonic microwave generation find applications in radio-over-fiber (RoF) technology that holds great promise for 4G mobile communications systems [23]. Both single-beam optically injected semiconductor lasers [21-25] and dual-beam optically injected semiconductor lasers [26-28] have been considered. Tunable narrow-linewidth microwave signals have been generated by using the period-one (P1) oscillations states that appear when the semiconductor laser is subject to a single-beam optical injection scheme [23]. Photonic microwaves from the P1 oscillation of an optically injected edge-emitter semiconductor laser have reached beyond 100 GHz [25]. The tuning range of the generated microwave signals is limited to several tens of GHz [27]. Recently a very high frequency (121.7 GHz) microwave signal has been generated by using a dual-beam optically injected semiconductor laser [27]. Experimental tuning ranges, limited by the bandwidth of the photodetector, around 20 GHz were demonstrated [27]. Numerical calculations have shown that a wide continuous tuning range of more than 100 GHz is obtained by adjusting the detuning frequency of the two master lasers [28].

In this work we study in a theoretical way the polarization and transverse mode properties of a multimode VCSEL when it is subject to two-frequency (or dual-beam) orthogonal optical injection. The dynamics of the two linear polarizations of two transverse modes of the VCSEL is found using the model of [13] extended to consider dual-beam orthogonal optical injection. We analyze the nonlinear dynamics of the system making special emphasis in the double injection locking observed at large injection strengths, useful for photonic microwave signal generation. In previous works using dual-beam optical injection a single mode slave edge emitter laser was considered [26-28]. Also both master and slave edge emitter lasers had parallel linear polarizations [26-28]. Simulation of single-transverse mode VCSELs with the extra degree of freedom given by the polarization of the device show that the double injection locking can be obtained when this device is subject to dual-beam orthogonal optical injection. Furthermore we consider multi-transverse mode VCSELs subject to the same type of optical injection. Again we obtain the double injection locking for this system. We show that the extra degree of freedom given by the multi-transverse mode operation of the VCSEL is useful for enhancing the performance of the photonic microwave generation system. In fact we obtain that the higher-order transverse mode is excited with much larger amplitudes than those obtained with a single-transverse mode VCSEL subject to the same dual-beam orthogonal optical injection. Wide tuning ranges and narrow linewidths are also demonstrated in our system.

Our paper is organized as follows. In Section II the theoretical model is presented. Section III is devoted to the single-transverse mode VCSEL subject to dual-beam orthogonal optical injection. In section IV we study the multi-transverse mode VCSEL subject to dual-beam orthogonal optical injection. Finally in section V we compare the results for single and multi-transverse mode case and finish with a summary and conclusions of the paper.

II. THEORETICAL MODEL

The theoretical model is based on a spatially dependent dynamical model of a multi-transverse mode VCSEL subject to orthogonal optical injection [13]. In this paper we extend it for considering a two-frequency optical injection. The simulated cylindrically symmetric weak index-guided structure, together with the complete details of the model can be found in [13]. Subscripts x and y will be used to denote the polarization direction. We will consider a small value of the index step (0.09) in such a way that the appropriate transverse modes of the structure are the LP_{mn} modes. Here we treat the case of VCSELs that can operate in the fundamental (LP_{01}) and in the first order (LP_{11}) transverse modes. Subscripts 0,1 will be used to denote the LP_{01} and LP_{11} modes, respectively. The equations describing the polarization and transverse mode behaviour of the VCSEL with a two-frequency orthogonal optical injection injected optical field read [13]:

$$\dot{E}_{0,x} = k(1+i\alpha)(E_{0,x}(g_{0,x}-1) + iE_{0,y}g_{0,xy}) - (\gamma_a + i\gamma_{p0})E_{0,x} + \sqrt{\frac{\beta}{2}}(\sqrt{N+\bar{n}}\xi_{0+}(t) + \sqrt{N-\bar{n}}\xi_{0-}(t))$$

$$\dot{E}_{0y} = k(1+i\alpha)(E_{0y}(g_{0y}-1) - iE_{0x}g_{0yx}) + (\gamma_a + i\gamma_{p0})E_{0y} + \frac{k_{01}}{\tau_{in}}e^{i\Delta\omega_1 t} + \frac{k_{02}}{\tau_{in}}e^{i\Delta\omega_2 t} - i\sqrt{\frac{\beta}{2}}(\sqrt{N+\bar{n}}\xi_{0+}(t) - \sqrt{N-\bar{n}}\xi_{0-}(t))$$

$$\dot{E}_{1x} = k(1+i\alpha)(E_{1x}(g_{1x} - \kappa_r) + iE_{1y}g_{1yx}) + i\gamma_p^r E_{1x} - (\gamma_a + i\gamma_{p1})E_{1x} + \sqrt{\frac{\beta}{2}}(\sqrt{N+\bar{n}}\xi_{1+}(t) + \sqrt{N-\bar{n}}\xi_{1-}(t))$$

$$\dot{E}_{1y} = k(1+i\alpha)(E_{1y}(g_{1y} - \kappa_r) - iE_{1x}g_{1yx}) + i\gamma_p^r E_{1y} + (\gamma_a + i\gamma_{p1})E_{1y} + \frac{k_{11}}{\tau_{in}}e^{i\Delta\omega_1 t} + \frac{k_{12}}{\tau_{in}}e^{i\Delta\omega_2 t} - i\sqrt{\frac{\beta}{2}}(\sqrt{N+\bar{n}}\xi_{1+}(t) - \sqrt{N-\bar{n}}\xi_{1-}(t))$$

$$\frac{\partial N(r,t)}{\partial t} = I(r) + D\nabla_{\perp}^2 N - \gamma_c \left[N \left(1 + \sum_{i=0,1} \sum_{j=x,y} |E_{ij}|^2 \psi_{ij}^2(r) \right) - in \sum_{i=0,1} (E_{ix}E_{iy}^* - E_{iy}E_{ix}^*) \psi_{ix}(r)\psi_{iy}(r) \right]$$

$$\frac{\partial n(r,t)}{\partial t} = -\gamma_s n + D\nabla_{\perp}^2 n - \gamma_c \left[n \sum_{i=0,1} \sum_{j=x,y} |E_{ij}|^2 \psi_{ij}^2(r) - iN \sum_{i=0,1} (E_{ix}E_{iy}^* - E_{iy}E_{ix}^*) \psi_{ix}(r)\psi_{iy}(r) \right]$$

where ψ_{0j} and ψ_{1j} are the modal profiles of the LP₀₁ and LP₁₁ modes obtained by solving the Helmholtz equation [29-30], respectively, E_{0j} and E_{1j} are the modal amplitudes of these modes, the subindex j stands for the linear polarization state of the given mode, $N(r,t)$ is the total carrier number and $n(r,t)$ is the difference in the carrier numbers of the two magnetic sublevels. κ_r is the relative loss of the LP₁₁ mode with respect to the LP₀₁ mode. That parameter determines the value of the injection current at which the LP₁₁ mode begins lasing. $I(r)$ represents a uniform current injection of over a circular disc of 6 μm radius, and then $I(r)=I$ if $r < 6 \mu\text{m}$, and $I(r)=0$, elsewhere. The normal gain normalized to the threshold gain, g_{ij} ($i=0,1$, $j=x, y$), and g_{ijk} ($i=0,1$; $jk=xy, yx$) are given by

$$g_{ij} = \frac{\int_0^{\infty} N(r,t) \psi_{ij}^2(r) r dr}{\int_0^{\infty} \psi_{ij}^2(r) r dr} \quad g_{i,jk} = \frac{\int_0^{\infty} n(r,t) \psi_{ij}(r) \psi_{ik}(r) r dr}{\int_0^{\infty} \psi_{ij}^2(r) r dr}$$

In the dual-beam injection scheme the VCSEL is optically injected by a master laser 1 (ML1) and a master laser 2 (ML2), with optical frequencies ω_1 and ω_2 , respectively. Two frequency detunings, $\Delta\omega_1 = \omega_1 - \omega_h$ and $\Delta\omega_2 = \omega_2 - \omega_h$, with respect to the central frequency between the two polarizations of the fundamental mode $\omega_h = (\omega_{0x} + \omega_{0y})/2$, appear in the equations. The injection terms only appear in the equations for E_{0y} and E_{1y} , hence linear optical injection in the y -direction is considered for both master lasers. In this way orthogonal optical injection is achieved if the free-running VCSEL emits only in the x -linear polarization, as it will be considered in this work. Optical injection terms are also characterized by the injection strengths, k_{ij} and the VCSEL roundtrip time, $\tau_{in} = 2L/v_g$, where v_g is the group velocity. The injection strength k_{im} ($i=0,1$, $m=1,2$) is given by

$$k_{im} = \left(\frac{1}{\sqrt{R}} - \sqrt{R} \right) \sqrt{\eta_{inj}} \sqrt{P_{inj,im}}$$

where R is the output-mirror reflectivity, η_{inj} is the coupling efficiency of the injected light to the optical field in the laser cavity and $P_{inj,im}$ is the power injected in the i -transverse mode by the m -master laser [31]. We choose the k_{im} values in this work in relation to what should be expected when light from a multi-transverse mode VCSEL is injected into a similar device. k_{01} (k_{12}) is related to the spatial overlap integral between the profiles of the fundamental modes (the higher-order modes) of master and slave lasers. Then a reasonable choice is $k_{01} = k_{12} = k_s$. k_{02} (k_{11}) is related to the spatial overlap integral between the profiles of the fundamental mode of the slave and the higher order mode of the master (higher-order mode of the slave and the fundamental mode of the master) VCSEL. In this way we choose $k_{02} = k_{11} = k_c$. The rest of the parameters that appear in the equations and their meaning are specified in the Table I. The frequency splitting between the orthogonal polarizations of the LP₀₁ mode, $2\gamma_{p0}/(2\pi)$, between the orthogonal polarizations of the LP₁₁ mode, $2\gamma_{p1}/(2\pi)$, and between the two transverse modes with the same polarization, $\gamma_p^r/(2\pi)$, are obtained from the calculation of the waveguide modes via the Helmholtz equation [29-30]. We have chosen the values of $n_{core,x}$, $n_{core,y}$ and n_{cladd} in such a way that $2\gamma_{p0}/(2\pi) = 10$ GHz and $\gamma_p^r/(2\pi) = 63$ GHz. Spontaneous emission noise processes are modeled by

the terms ξ_x taken as complex Gaussian white noise sources of zero mean and delta-correlated in time. In the noise terms, the carrier distribution is integrated over the active region:

$$\bar{N} = \frac{\int_0^a N(r,t) r dr}{a^2}, \quad \bar{n} = \frac{\int_0^a n(r,t) r dr}{a^2}$$

Time and space integration steps of 0.01 ps and 0.12 microns, respectively, have been used. The boundary conditions for the carrier distribution are taken as $N(\infty,t)=0$, $n(\infty,t)=0$. The initial conditions correspond to a below threshold stationary solution, i.e. to $I=0.1 I_{th}$, where I_{th} is the threshold current. We show in Fig. 1 the dynamical evolution of a free-running single-transverse mode VCSEL when switched-on at time $t>0$ with a $I=1.8 I_{th}$ bias current value. We have chosen a value $\kappa_x=3$ to assure fundamental transverse mode operation. The VCSEL emits in the steady state in the x-polarization with a single peaked RF spectrum appearing at the relaxation oscillation frequency. Optical spectrum in Fig. 1(c) show the 10 GHz frequency separation between $LP_{01,y}$ and $LP_{01,x}$.

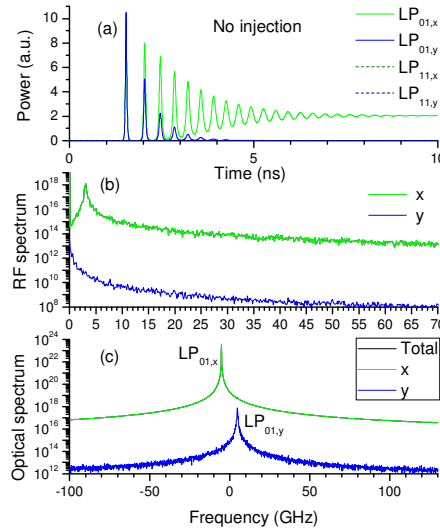


Fig. 1. Temporal and spectral dynamics of free-running single-transverse mode VCSEL (a) Time traces of the power of the polarized transverse modes. (b) RF spectra of the polarized powers. (c) Optical spectra of the x-polarized, y-polarized and total power.

SYMBOL	VALUE	MEANING OF THE SYMBOL
a	$6 \mu m$	Radius of the core region
L	$1 \mu m$	Length of the cavity
$n_{core,x}$	3.5001025	Refractive index of the core region in the x-direction
$n_{core,y}$	3.5	Refractive index of the core region in the y-direction
n_{cladd}	3.41	Refractive index of the cladding region
k	$300 ns^{-1}$	Field decay rate
α	3	Linewidth enhancement factor
γ_e	$0.55 ns^{-1}$	Decay rate for the total carrier population
γ_s	$1000 ns^{-1}$	Spin-flip relaxation rate
D	$10 cm^2 s^{-1}$	Diffusion coefficient
β	$10^{-5} ns^{-1}$	Spontaneous emission coefficient
γ_a	$-0.3 ns^{-1}$	Dichroism

Table 1. Device and material parameters

III. DUAL-BEAM OPTICALLY INJECTED SINGLE-TRANSVERSE MODE VCSEL

We now present the results corresponding to the orthogonal two-frequency optical injection on the single-transverse mode VCSEL simulated in the previous section. Results are given in terms of the separation between the frequencies of the two master lasers, $\Delta f = (\omega_2 - \omega_1)/(2\pi)$, the frequency detuning of ML1 with respect to the frequency of the $LP_{01,y}$ mode, $\Delta\nu$, and the injection strength κ_3 . In the calculations presented in this paper we consider a value of $\kappa_3 = \kappa_5/2$. In all the calculations we switch-on the laser applying a constant current of $1.8 I_{th}$ for $t > 0$. Orthogonal optical injection is applied for $t > 4$ ns. We let the system evolve during an additional transient time of 10 ns above which data are collected in order to calculate RF and optical spectra. Fig. 2(a) shows the results for a weak injection of $\kappa_3 = 10^{-5}$, with the frequency of ML1 just at the $LP_{01,y}$ mode frequency. A similar time evolution to that of the free-running VCSEL is obtained. The effects of the orthogonal injection are more clear in the spectra. In the y-polarized optical spectrum the peak corresponding to the $LP_{01,y}$ mode (at 5 GHz) is enhanced and a symmetric peak with respect to the $LP_{01,x}$ frequency appears at -15 GHz. The peak corresponding to the frequency of ML2 also appears at 105 GHz. The frequency separation between the first two peaks in the y-polarized spectrum is 20 GHz, that is the value of the frequency at which the RF spectrum of the y-polarization develops an additional peak. A peak also appears at 100 GHz, that is precisely the frequency separation between ML2 and ML1. An irregular dynamics is obtained when increasing κ_3 as illustrated in Fig. 2(b). PS has been achieved because almost all the power is y-polarized: the x-polarization only appears eventually with small power. This irregular dynamics is also characterized by the broadened optical and RF spectra. Further increase of κ_3 leads to a very interesting situation in which an almost sinusoidal time trace is obtained for the power of $LP_{01,y}$ mode. The frequency of this sinusoidal modulation is Δf . The optical spectrum consists on two well defined peaks at the ML1 and ML2 optical frequencies and the RF spectrum has a very narrow peak at Δf , the frequency separation between ML2 and ML1. This situation is similar to the double injection locking that has been described experimentally by Y. S. Juan using a single mode DFB laser subject to dual-beam injection [27]. Double injection locking has also been obtained in simulations using a single-mode rate equation model [28]. In [27-28] a linearly polarized single longitudinal mode is subject to a parallel polarized double-beam optical injection. The main difference of our results with respect to those in [27-28] lies in the consideration of the additional degree of freedom corresponding to the polarization: double injection locking can also be achieved when using orthogonally polarized dual-beam injection.

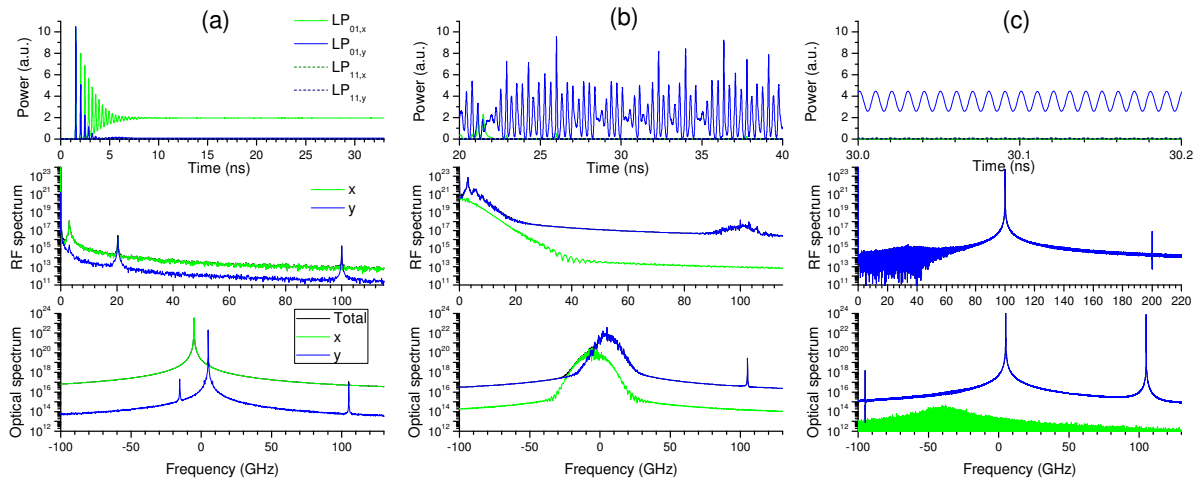


Fig. 2. Temporal and spectral dynamics of the single-transverse mode VCSEL when $\Delta f = 100$ GHz and $\Delta\nu = 0$ GHz, and (a) $\kappa_3 = 10^{-5}$, (b) $\kappa_3 = 2 \cdot 10^{-4}$, and (c) $\kappa_3 = 10^{-2}$. Upper row: Time traces of the power of the polarized transverse modes. Middle row: RF spectra of the polarized powers. Lower row: optical spectra of the x-polarized, y-polarized and total power.

Wide tunability of the microwave signal generated by dual-beam optical injection was shown in [27-28]. Numerical simulations showed that the frequency of the generated microwave signal can be tuned continuously up to 120 GHz [28]. Fig. 3 shows that our system also shows wide tunability. Results are shown for several values of Δf , from below the transverse mode separation (Fig. 3a), at the transverse mode separation (Fig. 3b) and well above the transverse mode

separation (Fig. 3c). In all the cases well defined sinusoidal time traces are obtained for the power of the $LP_{01,y}$ mode. The amplitude of the oscillations decreases as Δf increases. All the RF spectra show a narrow peak at the Δf frequency, even at the very large values simulated in Fig. 3(c), well beyond the microwave range. The continuous character of the tunability of the system and the range of Δf frequencies in which appreciable amplitudes of the signal are achieved will be analyzed at the end of Section IV.

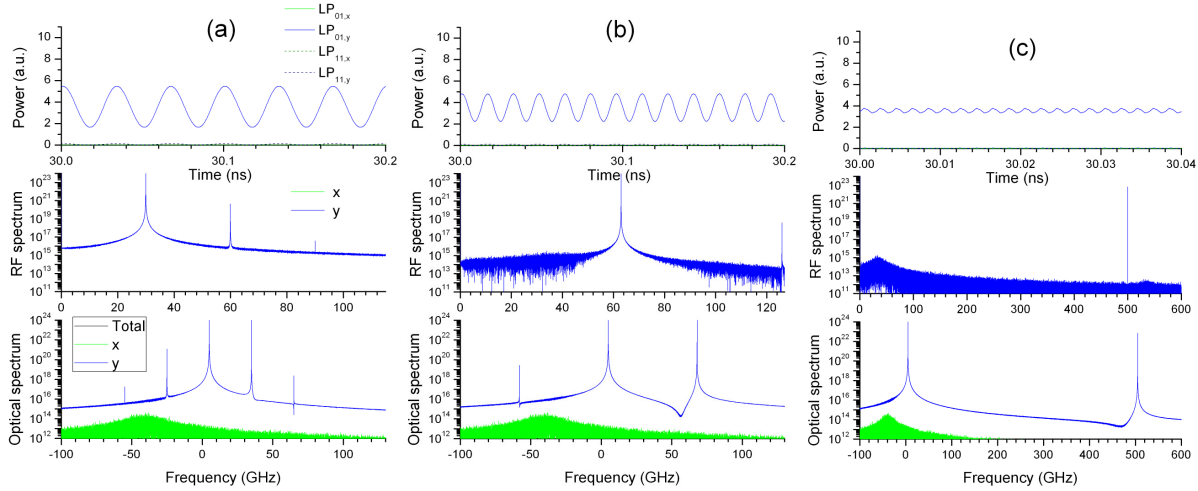


Fig. 3. Temporal and spectral dynamics of the single-transverse mode VCSEL when $\Delta f = 30, 63$ and 500 GHz and $\Delta\nu = 0$ GHz, $\kappa_s = 10^{-2}$. Upper row: Time traces of the power of the polarized transverse modes. Middle row: RF spectra of the polarized powers. Lower row: optical spectra of the x-polarized, y-polarized and total power.

IV. DUAL-BEAM OPTICALLY INJECTED MULTI-TRANSVERSE MODE VCSEL

In this section we present the results corresponding to the orthogonal two-frequency optical injection on a multi-transverse mode VCSEL. The multi-transverse mode VCSEL that is simulated is exactly the same than that of the previous section but changing the parameter κ_r to a smaller value for which both transverse modes have rather similar losses. Results obtained for $\kappa_r = 1.022$ when the VCSEL is not subject to optical injection ($\kappa_s = \kappa_r = 0$) are plotted in Fig. 4. The free-running VCSEL shows a steady-state in which both transverse modes, LP_{01} and LP_{11} , are excited in the x-direction. The steady-state total power in Fig. 4(a) is 1.7, a similar value to the value 2 that was obtained for Fig. 1(a). The power in $LP_{11,x}$ is only slightly larger than that of $LP_{01,x}$. Fig. 4(b) shows that the x-polarized RF spectrum has two peaks that appear due to the multi-transverse mode character of the VCSEL [32-34]. Linearization of the stochastic rate equations around an analytical steady state solution [35] has shown that the relative intensity noise in multi-transverse modes have resonance peaks that appear at frequencies that correspond to the relaxation oscillation frequencies of the multimode laser [34]. The multimode character of the systems is also clear from the optical spectra of Fig. 4(c). The separation between $LP_{01,x}$ and $LP_{11,x}$, similar to the separation between $LP_{01,y}$ and $LP_{11,y}$, is around 63 GHz.

Fig. 5 shows the results of the multi-transverse mode VCSEL subject to orthogonal dual-beam optical injection. The levels of the injection strength, Δf and $\Delta\nu$ are equal to those considered in the single-transverse mode case (Fig. 2). In this way we will be able to compare the performance of microwave generating systems using single and multi-transverse mode VCSELs. Fig. 5(a) shows the results for a weak injection of $\kappa_s = 10^{-5}$, with the frequency of ML1 just at the $LP_{01,y}$ mode frequency. Rather similar time evolution to that of the free-running VCSEL is obtained with some new characteristic features. Some power appears in the $LP_{01,y}$ mode with a corresponding decrease in the power of the $LP_{01,x}$ mode. The optical spectrum shows that the peak corresponding to the $LP_{01,y}$ mode (at 5 GHz) is enhanced and a small symmetric peak with respect to the $LP_{01,x}$ frequency appears at -15 GHz. Two other strong peaks appear in that spectrum: the first, near 70 GHz, corresponds to $LP_{11,y}$ mode and the second one, near 105 GHz, appears at the ML2 frequency. Frequency differences between those peaks explain the multi-peaked structure of the y-polarized RF spectrum. A regular dynamics involving $LP_{01,y}$ and $LP_{11,x}$ is obtained when increasing κ_s as illustrated in Fig. 5(b), in contrast to the irregular

dynamics of Fig. 2(b). A complete PS has not been achieved yet in contrast to Fig. 5(c) for which the increase of injection strength has resulted in the complete disappearance of the x-polarized power.

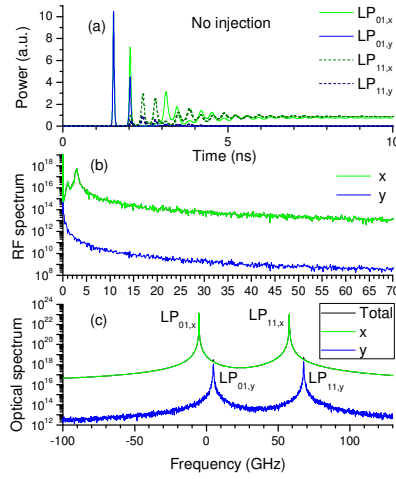


Fig. 4. Temporal and spectral dynamics of free-running multi-transverse mode VCSEL. (a) Time traces of the power of the polarized transverse modes. (b) RF spectra of the polarized powers. (c) Optical spectra of the x-polarized, y-polarized and total power.

Similarly to Fig. 2(c), Fig. 5(c) also shows the double injection locking phenomenon. Again, two well defined peaks at the frequencies of ML1 and ML2 are observed in the y-polarized optical spectrum resulting in a RF spectrum with a narrow peak at the Δf frequency. But Fig. 5(c) also shows an interesting and novel feature when compared to Fig. 2(c): the high-order transverse mode $LP_{11,y}$ is excited with a much larger amplitude than that of the $LP_{01,y}$ mode. The power of both transverse modes oscillate with a $\sim\pi/2$ phase difference. The variation of the total power is nearly sinusoidal, as shown in the RF spectrum of Fig. 5(c). Interestingly, the amplitude of the total power is much larger than the one obtained with the equivalent single-transverse mode VCSEL case illustrated in Fig. 2(c). This shows that the amplitude of the microwave signal generated by double-beam optical injection is enhanced if multi-transverse mode operation in the VCSEL is considered instead of single-transverse mode operation.

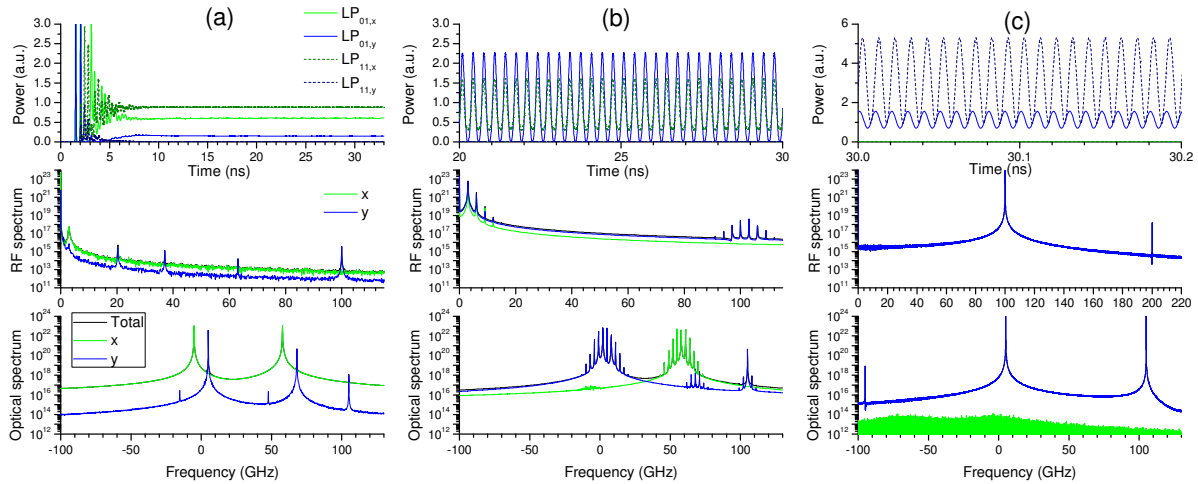


Fig. 5. Temporal and spectral dynamics of the multi-transverse mode VCSEL when $\Delta f=100$ GHz and $\Delta\nu=0$ GHz, (a) $\kappa_s=10^{-5}$, (b) $\kappa_s=2 \cdot 10^{-4}$, and (c) $\kappa_s=10^{-2}$. Upper row: Time traces of the power of the polarized transverse modes. Middle row: RF spectra of the polarized powers. Lower row: optical spectra of the x-polarized, y-polarized and total power.

We now analyze the effect of the frequency detuning, $\Delta\nu$, on the dynamics of the system. Fig. 6 shows the results obtained when $\Delta\nu=-5$ GHz. When the strength of the optical injection is weak ($\kappa_i=10^{-5}$), the time traces of Fig. 6(a) show that the dynamics of $LP_{01,x}$ and $LP_{11,x}$ are less affected by the injection than for the $\Delta\nu=0$ GHz case. Y-polarized optical spectrum show peaks corresponding to the optical injection given by ML1 and ML2 that appear at 0 and 100 GHz, respectively. Increasing the injection strength leads to in-phase oscillations of $LP_{01,x}$ and $LP_{11,x}$ and a small oscillation of the $LP_{01,y}$ power, as it can be seen in Fig. 6(b). Fig. 6(c) illustrates the dynamics when $\kappa_i=10^{-2}$. The dynamical evolution and optical spectra are very similar to those shown in Fig. 5(c). Only the expected shift in the y-polarized optical spectrum with respect to Fig. 5(c) is observed because now the light emitted by ML1 is injected at -5 GHz with respect to the free-running $LP_{01,y}$ frequency.

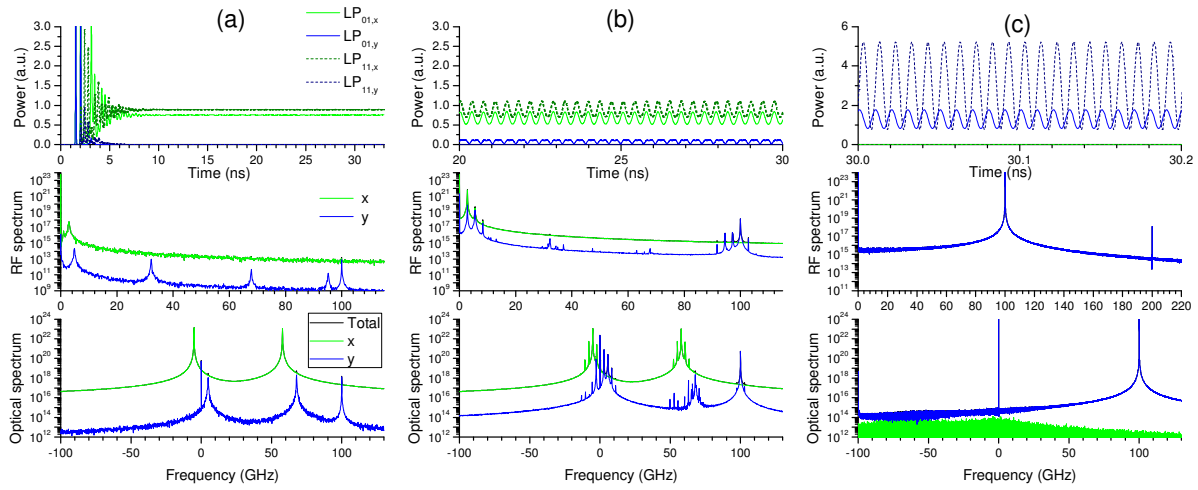


Fig. 6. Temporal and spectral dynamics of the multi-transverse mode VCSEL when $\Delta f=100$ GHz and $\Delta\nu=-5$ GHz (a) $\kappa_i=10^{-5}$, (b) $\kappa_i=2 \cdot 10^{-4}$, and (c) $\kappa_i=10^{-2}$. Upper row: Time traces of the power of the polarized transverse modes. Middle row: RF spectra of the polarized powers. Lower row: optical spectra of the x-polarized, y-polarized and total power.

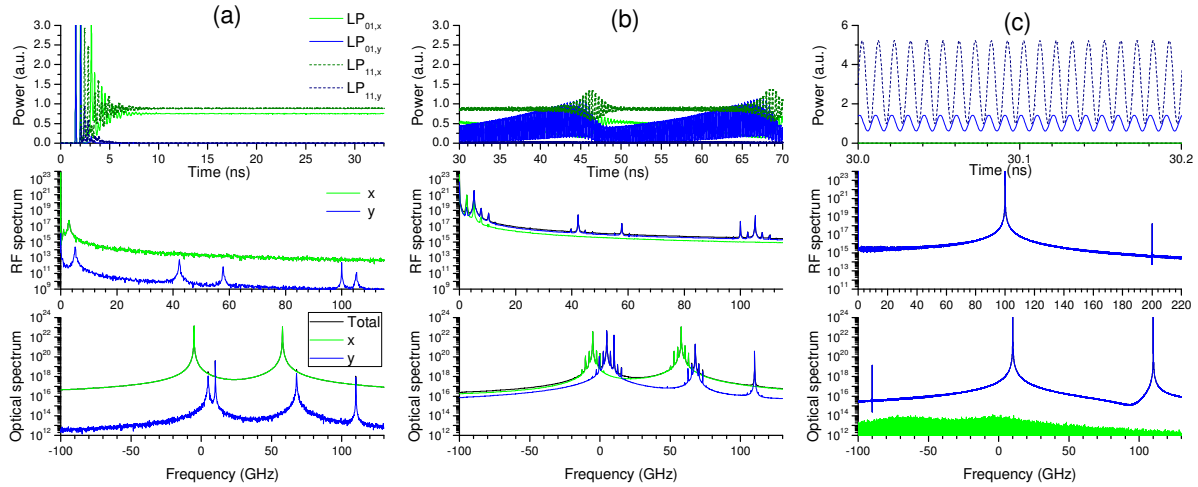


Fig. 7. Temporal and spectral dynamics of the multi-transverse mode VCSEL when $\Delta f=100$ GHz and $\Delta\nu=5$ GHz, (a) $\kappa_i=10^{-5}$, (b) $\kappa_i=2 \cdot 10^{-4}$, and (c) $\kappa_i=10^{-2}$. Upper row: Time traces of the power of the polarized transverse modes. Middle row: RF spectra of the polarized powers. Lower row: optical spectra of the x-polarized, y-polarized and total power.

Results obtained when $\Delta\nu=5$ GHz are shown in Fig. 7. For weak injection strength ($\kappa_s=10^{-5}$), time traces are very similar to those plotted in Fig. 6(a). The y-polarized optical spectrum is such that the peaks corresponding to ML1 and ML2 appear at 10 and 110 GHz, respectively. Fig. 7(b) shows results obtained for $\kappa_s=2 \cdot 10^{-4}$. A more complicated periodic dynamical evolution is obtained than in Fig. 6(b). $LP_{01,x}$, $LP_{11,x}$, and $LP_{01,y}$ modes participate in the dynamics with appreciable power. The $LP_{01,y}$ mode has much more power than for the $\Delta\nu=5$ GHz case. Fig. 7(c) shows that the dynamics obtained when $\kappa_s=10^{-2}$ is very similar to that shown in Figs. 5(c) and 6(c). This indicates that there is an appreciable range of $\Delta\nu$ for which the enhancement of the amplitude of the generated microwave signal due to high-order transverse mode excitation does not depend on the $\Delta\nu$ value.

We now discuss quantitatively this enhancement and the tunability of our system. Fig. 8 shows the peak-to-peak amplitude of the total power as a function of the frequency difference between ML2 and ML1, that is the frequency of the generated microwaves, Δf . Results for single and multi-transverse mode VCSELs are included. Also results for two injection strength levels are shown. All the cases reported in this figure have an almost sinusoidal variation of the total power. Peak-to-peak amplitudes decrease as Δf increases. An increase of the injection strength κ_s leads to larger peak-to-peak amplitudes for both, single and multi-transverse mode cases. For all the values of Δf and κ_s the amplitude of the oscillation obtained with multi-transverse mode VCSELs is larger than that obtained for single-transverse mode VCSELs. The ratio between both amplitudes varies between 2 and 2.6 for the cases considered in Fig. 8. The 2.6 value is obtained for $\kappa_s=10^{-2}$ and $\Delta f=65$ GHz, value that is almost similar to the transverse mode separation. This indicates that the maximum enhancement is obtained when the optical frequencies of ML1 and ML2 coincide with the frequencies of the free-running $LP_{01,y}$, and $LP_{11,y}$ modes, respectively.

Figure 8 also shows that larger variations of peak-to-peak amplitudes as Δf change occur in the microwave region (<300 GHz). In the graph we have also considered a Δf range that goes beyond the microwave range. In this region the generated radiation has an appreciable amplitude that increases as κ_s is increased. The amplitude of this modulation slightly decreases when Δf is in the THz region.

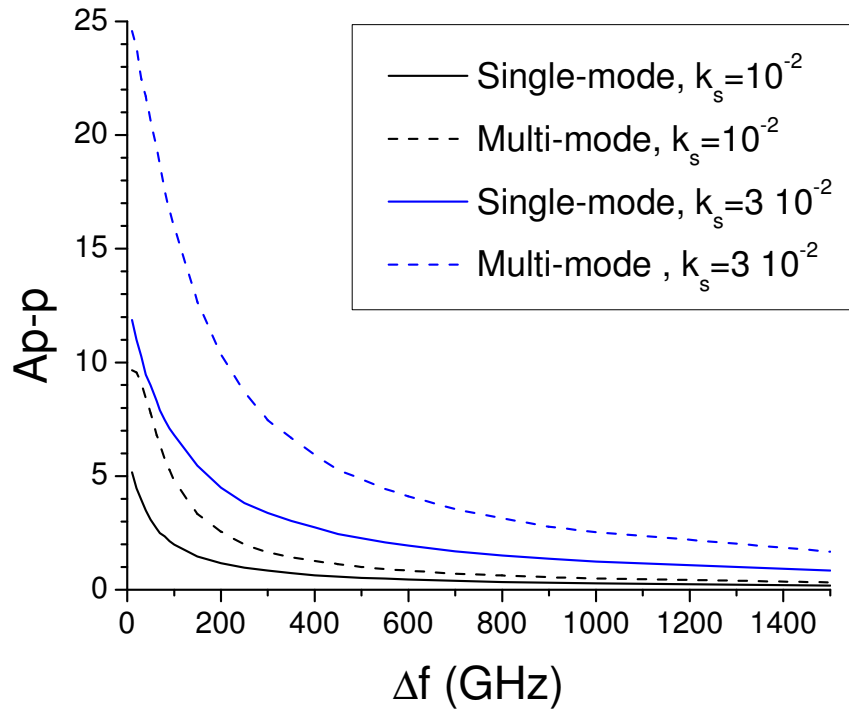


Fig. 8. Peak-to-peak amplitude, A_{p-p} , of the total power as a function of the generated frequency, Δf . In this Figure $\Delta\nu=0$ GHz

We have also made a preliminar analysis of the linewidths of the high-frequency signals generated by double-injection locked single and multi-transverse mode VCSELs. For instance 3-dB linewidths of 5 and 4.4 MHz are obtained for Fig. 2(c) and Fig. 5(c), respectively. Narrow linewidths, similar to the values found in [27] and [28], 6 and 19 MHz, respectively, are demonstrated. We have also made a preliminary analysis of the relative phase between power time series corresponding to $LP_{01,y}$ and $LP_{11,y}$ in the double-injection locked multi-transverse mode VCSEL case. The relative phase can change depending on the injection conditions, in fact it decreases as the value of the κ_i injection strength increases. Further work is intended to analyze these points in a more systematic way.

V. SUMMARY AND CONCLUSIONS.

In this work we have made a theoretical study of the polarization and transverse mode properties of single and multi-transverse mode VCSELs when they are subject to dual-beam orthogonal optical injection. We have focused our analysis in the double injection locking observed at large injection strengths, useful for photonic microwave signal generation. Numerical simulations of single and multi-transverse mode VCSELs have shown that the double injection locking can be obtained when these devices are subject to dual-beam orthogonal optical injection. We have shown that the response of multi-transverse mode VCSELs under dual-beam orthogonal optical injection is larger than that obtained with similar single-transverse mode VCSELs: In this way an enhancement of the performance of the photonic microwave generation system based on dual-beam optical injection is obtained when using multi-transverse mode VCSELs. Wide tuning ranges, beyond the THz region, and narrow linewidths are also demonstrated in our system.

ACKNOWLEDGEMENTS

The authors acknowledge support from the Ministerio de Ciencia e Innovación under project TEC2009-14581-C02-02. AQ was supported in part by the Fondo Social Europeo (FSE) under the programme Junta de Ampliación de Estudios (JAE-predoc) programme.

REFERENCES

- [1] J. Ohtsubo, "Semiconductor lasers. Stability, instability and chaos". Springer series in optical sciences. Berlin 2007.
- [2] F. Koyama, "Recent advances of VCSEL Photonics," *J. Lightwave Technol.* vol. 24, no. 12, pp. 4502-4513, Dec. 2006.
- [3] C. H. Chang, L. Chrostowski, C. J. Chang-Hasnain, "Injection locking of VCSELs," *IEEE J. Select. Topics Quantum Electron.*, vol. 9, no. 5, pp.1386-1393, Sep./Oct 2003.
- [4] D. Parekh, X. Zhao, W. Hofmann, M. C. Amann, L. A. Zenteno and C. J. Chang-Hasnain, "Greatly enhanced modulation response of injection-locked multimode VCSELs," *Opt. Exp.*, vol. 16, no. 26, pp. 21582-21586, Dec. 2008.
- [5] H. Li, T. Lucas, J. G. McInerney, M. Wright, and R. A. Morgan, "Injection locking dynamics of vertical cavity semiconductor lasers under conventional and phase conjugate injection." *IEEE J. Quantum Electronics*, vol. 32, no. 3, pp. 227-235, Feb. 1996.
- [6] Z. G. Pan, S. Jiang, M. Dagenais, R. A. Morgan, K. Kojima, M. T. Asom, and R. E. Leibenguth, "Optical injection induced polarization bistability in vertical-cavity surface-emitting lasers," *Appl. Phys. Lett.*, vol. 63, no. 22, pp. 2999-3001, Nov.1993.
- [7] Y. Hong, K.A. Shore, A. Larsson, M. Ghisoni, and J. Halonen, "Pure frequency-polarisation bistability in vertical-cavity surface-emitting lasers subject to optical injection", *Electron. Lett.* 36, no. 24, pp. 2019-2020, 2000.
- [8] J. Buesa, I. Gatara, K. Panajotov, H. Thienpont, and M. Sciamanna, "Mapping of the dynamics induced by orthogonal optical injection in vertical-cavity surface-emitting lasers", *IEEE J. Quantum Electron.*, vol. 42, no. 2, pp. 198-207, Feb. 2006.

- [9] K. Panajotov, I. Gatare, A. Valle, H. Thienpont and M. Sciamanna, "Polarization- and Transverse-Mode Dynamics in Optically Injected and Gain-Switched Vertical-Cavity Surface-Emitting Lasers", *IEEE J. Quantum Electron.* vol.45, no.11, pp.1473-1481, Nov. 2009.
- [10] A. Valle, M. Gomez-Molina, and L. Pesquera, "Polarization bistability in 1550 nm wavelength single-mode vertical-cavity surface-emitting lasers subject to orthogonal optical injection," *IEEE J. Sel. Top in Quantum Electron.*, vol. 14, no. 3, pp. 895-902, May/Jun.2008.
- [11] A. Hurtado, I. D. Henning, and M. J. Adams, "Two-wavelength switching with a 1550 nm VCSEL under single orthogonal optical injection," *IEEE J. Sel. Top. in Quantum Electron*, vol. 14, no. 3, pp. 911-917, May/Jun.2008.
- [12] K. H. Jeong, K. H. Kim, S. H. Lee, M. H. Lee, B. S. Yoo and K. A. Shore, "Optical injection-induced polarization switching dynamics in 1.5 μm wavelength single-mode vertical-cavity surface-emitting lasers," *IEEE Photon. Technol. Lett.*, vol. 20, no. 9-12, pp. 779-781, May. 2008.
- [13] A. Valle, I. Gatare, K. Panajotov, and M. Sciamanna, "Transverse mode switching and locking in vertical-cavity surface-emitting lasers subject to orthogonal optical injection", *IEEE J. Quantum Electron.* vol.43, no. 4, pp.322-333, Apr. 2007.
- [14] A. Quirce, J.R. Cuesta, A. Valle, A. Hurtado, L. Pesquera, and M. J. Adams, "Polarization bistability induced by orthogonal optical injection in 1550-nm multimode VCSELs", *IEEE J. Sel. Top. in Quantum Electron.*, vol. 18, no. 2, pp. 772-778, Mar. 2012.
- [15] H. Lin, Y. Zhang, D. W. Pierce, A. Quirce, and A. Valle, "Polarization dynamics of a multimode vertical-cavity surface-emitting laser subject to orthogonal optical injection", *J. Opt. Soc. Am. B*, in press, 2012.
- [16] C. J. Chang-Hasnain, J. P. Harbison, G. Hasnain, A. C. Von Lehmen, L. T. Florez, and N. G. Stoffel, "Dynamic, polarization and transverse mode characteristics of vertical-cavity surface-emitting lasers", *IEEE J. Quantum Electron.*, vol. 27, no. 6, pp. 1402-1409, Jun. 1991.
- [17] A. Valle, J. Sarma, K. A. Shore, "Spatial holeburning effects on the dynamics of vertical cavity surface-emitting laser diodes", *IEEE J. Quantum Electron.*, vol. 31, no. 8, pp. 1423-1431, Aug. 1995.
- [18] K. D. Choquette, R. P. Schneider, K. L. Lear, and R. E. Leibenguth, "Gain-dependent polarization properties of vertical-cavity lasers", *IEEE J. Select. Topics Quantum Electron.*, vol. 1, no. 2, pp. 661-666, Mar./Apr 1995.
- [19] A. Hayat, A. Bacou, A. Rissons, J.C. Mollier, V. Iakovlev, A. Sirbu, and E. Kapon, "Long-wavelength VCSEL-by-VCSEL optical injection locking", *IEEE Trans. Microw. Theory and Techniques*, vol. 57, no. 7, pp. 1850-1858, Jul. 2009.
- [20] H. Lin, D.W. Pierce, A.J. Basnet, A. Quirce, Y. Zhang, and A. Valle, "Two-frequency injection on a multimode vertical-cavity surface-emitting laser", *Opt. Exp.*, vol. 19, no. 23, pp. 22437-22442, 2011.
- [21] S. C. Chan, R. Diaz, J. M. Liu, "Novel photonic applications of nonlinear semiconductor laser dynamics", *Opt. Quant. Electron.*, vol. 40, no 2-4, pp. 83-95, 2008.
- [22] S.C. Chan, S.K. Hwang, and J. M. Liu, "Radio-over fiber transmission from an optically injected semiconductor laser in period-one state", *Opt. Exp.*, vol. 15, pp. 14921-14935, 2007.
- [23] X. Q. Qi, and J. M. Liu, "Photonic microwave applications of the dynamics of semiconductor lasers", *IEEE J. Sel. Top. in Quantum Electron.*, vol. 17, no. 5, pp. 1198-1211, 2011.
- [24] S. C. Chan, "Analysis of an optically injected semiconductor laser for microwave generation", *IEEE J. Quantum Electron.* vol. 46, no. 3, pp. 421-428, Mar. 2010.
- [25] S. C. Chan, S.K. Hwang, and J. M. Liu, "Radio-over-fiber AM-to-FM upconversion using an optically injected semiconductor laser", *Opt. Lett.*, vol. 31, pp. 2254-2256, Aug. 2006.
- [26] X. Q. Qi, and J. M. Liu, "Dynamic scenarios of dual-beam optically injected semiconductor lasers", *IEEE J. Quantum Electron.* vol. 47, no. 6, pp. 762-769, Jun. 2011.
- [27] Y. S. Juan, F. Y. Lin, "Photonic generation of broadly tunable microwave signals utilizing a dual-beam optically injected semiconductor laser", *IEEE Phot. Journal*, vol. 3, no. 4, pp. 644-650, Aug. 2011.
- [28] Y. C. Chen, Y. S. Juan, and F. Y. Lin, "High-frequency microwave signal generation in a semiconductor laser under double injection locking", *Proc. of SPIE*, vol. 7936, 793609, 2011.
- [29] A. Valle, K. A. Shore, and L. Pesquera, "Polarization selection in birefringent vertical cavity surface emitting lasers", *J. of Lightwav. Technol.*, vol. 14, no. 9, pp. 2062-2068, Aug. 1996.
- [30] A. Valle, J. Martin-Regalado, L. Pesquera, S. Balle, and M. San Miguel, "Polarization dynamics of birefringent index-guided vertical cavity surface emitting lasers", *Proc. of SPIE*, vol. 3282, pp. 280-291, 1998.
- [31] G. H. M. Van Tartwijk, and D. Lenstra, "Semiconductor lasers with optical injection and feedback", *Quantum Semiclass. Opt.*, vol.7, no. 2, pp. 87-143, 1995.

- [32] J. Dellunde, A. Valle, L. Pesquera, K. A. Shore, "Transverse-mode selection and noise properties of external-cavity surface-emitting lasers including multiple reflection effects", *J. Opt. Soc. Am B*, vol. 16, no. 11, pp. 2131-2139, 1999.
- [33] A. Valle, L. Pesquera, "Relative intensity noise of multitransverse-mode vertical-cavity surface-emitting lasers", *IEEE Phot. Technol. Lett.*, vol. 13, no. 4, pp. 272-274, 2001.
- [34] A. Valle, L. Pesquera, "Theoretical calculation of relative intensity noise of multimode vertical-cavity surface-emitting lasers", *IEEE J. Quantum Electron.* vol. 40, no. 6, pp. 597-606, Jun. 2004.
- [35] A. Valle, L. Pesquera, "Analytical calculation of transverse mode characteristics in vertical-cavity surface-emitting lasers", *J. Opt. Soc. Am B*, vol. 19, no. 7, pp. 1549-1557, 2002.